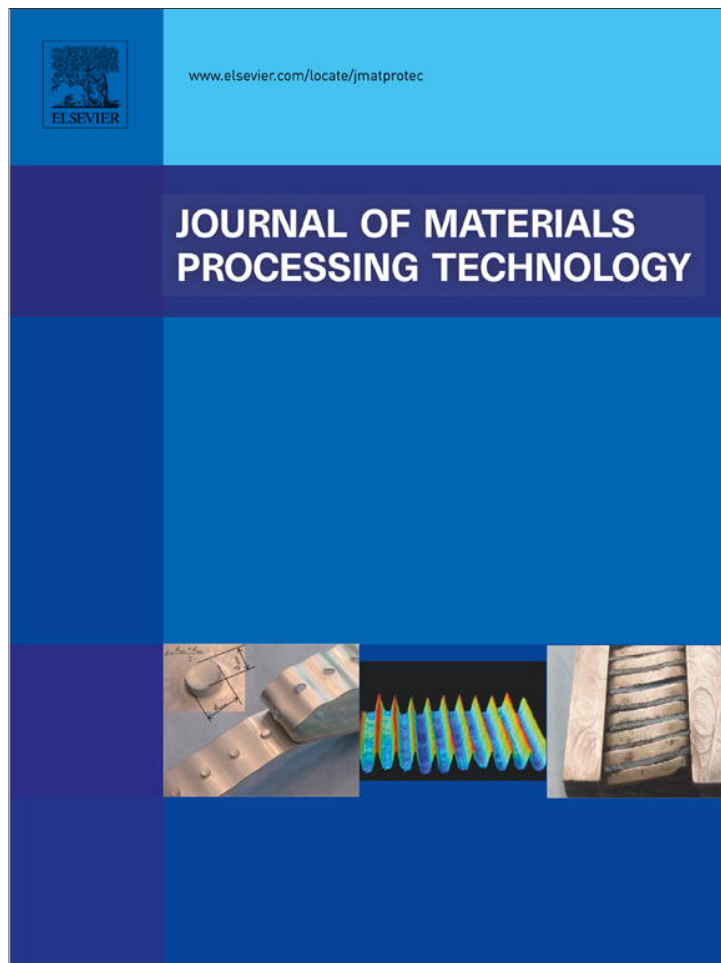


Provided for non-commercial research and education use.  
Not for reproduction, distribution or commercial use.



(This is a sample cover image for this issue. The actual cover is not yet available at this time.)

**This article appeared in a journal published by Elsevier. The attached copy is furnished to the author for internal non-commercial research and education use, including for instruction at the authors institution and sharing with colleagues.**

**Other uses, including reproduction and distribution, or selling or licensing copies, or posting to personal, institutional or third party websites are prohibited.**

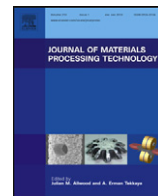
**In most cases authors are permitted to post their version of the article (e.g. in Word or Tex form) to their personal website or institutional repository. Authors requiring further information regarding Elsevier's archiving and manuscript policies are encouraged to visit:**

**<http://www.elsevier.com/copyright>**



Contents lists available at SciVerse ScienceDirect

## Journal of Materials Processing Technology

journal homepage: [www.elsevier.com/locate/jmatprotec](http://www.elsevier.com/locate/jmatprotec)

## Simulation of the transformation of iron intermetallics during homogenization of 6xxx series extrudable aluminum alloys

G.N. Haidemenopoulos\*, H. Kamoutsi, A.D. Zervaki

Department of Mechanical Engineering, University of Thessaly, Volos 38334, Greece

## ARTICLE INFO

## Article history:

Received 25 April 2012

Received in revised form 29 June 2012

Accepted 30 June 2012

Available online xxx

## Keywords:

Aluminum alloys

Intermetallics

Simulation of transformation

Homogenization

## ABSTRACT

A computational simulation of the  $\beta$ -AlFeSi to  $\alpha$ -AlFeSi transformation has been performed in this work by integrating the process steps of solidification and homogenization. The composition profiles of alloying elements as well as the profiles of weight fractions of all solid phases computed after solidification were entered as input for the simulation of the homogenization process which involves the dissolution of the  $Mg_2Si$  and the transformation of  $\beta$ -AlFeSi to  $\alpha$ -AlFeSi intermetallics.

The transformation fraction was computed as a function of homogenization temperature and time and the transformation kinetics compares well with published experimental data. The evolution of  $\alpha$ -AlFeSi weight fraction profile and the effect of grain size on transformation kinetics were also computed.

© 2012 Elsevier B.V. All rights reserved.

## 1. Introduction

One of the most important processes which takes place during the homogenization of commercial extrudable 6xxx series aluminum alloys, besides the dissolution of  $Mg_2Si$ , is the transformation of  $\beta$ -Al<sub>5</sub>FeSi to  $\alpha$ -Al<sub>12</sub>(Fe<sub>x</sub>Mn<sub>(1-x)</sub>)<sub>3</sub>Si (from now on  $\alpha$ -AlFeSi and  $\beta$ -AlFeSi or simply  $\alpha$  and  $\beta$ ). The  $\beta$ -AlFeSi has a monoclinic crystal structure and a plate-like morphology while the  $\alpha$ -AlFeSi has a cubic crystal structure and a globular morphology. The plate-like morphology of the  $\beta$ -AlFeSi phase limits the extrudability of the alloy since it induces local cracking and surface defects in the extruded material, while the presence of the more rounded  $\alpha$ -AlFeSi phase improves the extrudability of the alloy as discussed by Liu and Kang (1997). Furthermore it has been discussed by Cai et al. (2002) as well as by Kuijpers (2004) that the dissolution of the  $Mg_2Si$  phase is fast compared with the  $\beta \rightarrow \alpha$  transformation. Therefore the homogenization time adopted in industrial practice is controlled by the  $\beta \rightarrow \alpha$  transformation kinetics. Several experimental and theoretical investigations on Fe intermetallics in extrudable aluminum alloys have been performed. Mrówka-Nowotnik and Wierzbińska (2007) discuss the formation of Fe intermetallics during casting. Onurlu and Tekin (1994) studied the effect of heat treatment on the transformation  $\beta \rightarrow \alpha$  experimentally on a 6063 alloy. They determined that the transformation proceeded at a higher rate the higher the homogenization temperature. Tanihata et al. (1999) also investigated

experimentally the transformation  $\beta \rightarrow \alpha$  in 6063 alloys containing different amounts of Fe. In addition to experiments, modeling work has been performed by Kuijpers et al. (2003a). They developed a finite element model for the description of transformation kinetics at the early stages of the transformation as a function of homogenization temperature, as-cast microstructure and concentration of alloying elements. They validated their model with experimental data from a 6005 Al alloy and they concluded that the model is capable to predict the transformation fraction up to 50%. In a subsequent work Kuijpers et al. (2005) compared their model against experimental data from a series of Al–Mg–Si alloys containing different amounts of Mn and Si, in order to study the effect of Mn and Si on the transformation rate. They found that Si has a modest effect while Mn has a larger effect on the transformation rate. The model was capable to predict the transformation up to 4 h of homogenization time. Despite these efforts, a computational model of the transformation, covering the full range of industrial homogenization times (up to 10 h) does not exist. The aim of the present work is to simulate the  $\beta \rightarrow \alpha$  transformation by employing computational thermodynamics and kinetics. The usefulness of this work is that the simulation covers the microsegregation and associated precipitation of the Fe intermetallics during solidification of the aluminum billets as well as the full homogenization process including the dissolution and re-precipitation of  $Mg_2Si$  in addition to the  $\beta \rightarrow \alpha$  transformation. Predictions of the current simulation are compared against published experimental data from the work of Kuijpers et al. (2005) for the 6063 alloy. The effects of homogenization temperature and as-cast grain size are investigated. It should be mentioned that in a previous work by our group (Samaras and Haidemenopoulos, 2007) a simulation of the

\* Corresponding author. Tel.: +30 2421074062; fax: +30 2421074061.  
E-mail address: [hgreg@mie.uth.gr](mailto:hgreg@mie.uth.gr) (G.N. Haidemenopoulos).

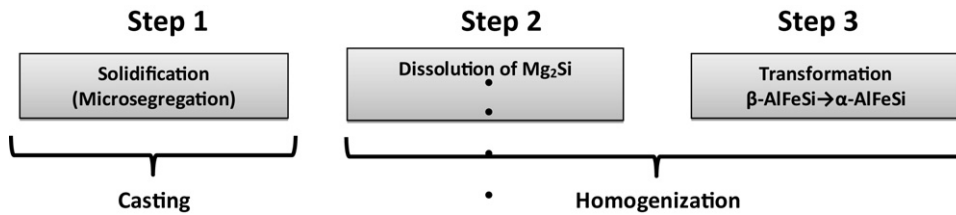


Fig. 1. Sequence of calculation steps.

homogenization of 6061 alloy was presented, regarding the dissolution and re-precipitation of Mg<sub>2</sub>Si, in which the β → α transformation was not included. Therefore the present work is a continuation of that study in order to describe the β → α transformation.

## 2. Methodology

The solution strategy is presented in this section. The specific details of each calculation including assumptions are presented in Section 3.

The simulation was carried out in three steps as follows (see Fig. 1):

- Step 1: solidification and microsegregation.
- Step 2: homogenization–dissolution of Mg<sub>2</sub>Si.
- Step 3: homogenization–transformation of β-AlFeSi to α-AlFeSi.

These steps were linked in the following sense. The output of step 1 were the profiles of weight fractions of intermetallic phases forming during solidification as well as the profiles of alloying elements in the FCC Al matrix phase. These microsegregation profiles represent the as-cast microstructure and were entered as input for the calculations in step 2 for the simulation of the dissolution of Mg<sub>2</sub>Si during homogenization. Once the dissolution of Mg<sub>2</sub>Si is complete, the simulation stops and the new composition profiles at the end of step 2 are calculated. These were used as input for the calculations in step 3, dealing with the β → α transformation. The computational thermodynamics package Thermo-Calc, described by Andersson et al. (2002) was used for step 1 calculations. Solidification was assumed to take place under the condition of limited diffusion in the solid (Scheil–Gulliver condition). The Thermo-Calc package can treat these problems with the build-in Scheil-module. Homogenization calculations, which involve diffusion, in steps 2 and 3, were treated with the computational kinetics package DICTRA, which is described by Borgenstam et al. (2000). In DICTRA the diffusion coefficients of alloying elements are temperature and composition-dependent. A geometrical model (to be described in detail in Section 3.2) was constructed for the description of the as-cast microstructure. Grain size and volume fractions of phases (resulting from step 1) were used as input for the construction of this model.

The alloy composition used for the present study is the same as the one used by Kuijpers et al. (2005) and is Al–0.43Mg–0.58Si–0.18Fe–0.02Mn (wt%).

## 3. Results and discussion

### 3.1. Solidification and microsegregation (step 1)

The aim of this step was to compute the weight fractions of phases and composition profiles of alloying elements (microsegregation) resulting from the solidification of the 6063 alloy. These results represent the as-cast microstructure.

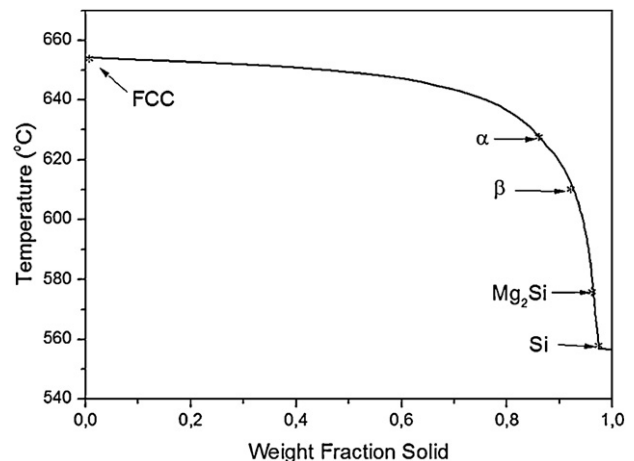


Fig. 2. Solidification path of 6063 alloy. Arrows indicate the formation of solid phases.

Microsegregation in aluminum is a result of the low solubility of the alloying elements in the solid in relation with the liquid. The low aluminum solid solubility leads to the formation of secondary phases in the as-cast microstructure. The size and morphology of these phases depends on the chemical composition, the dendrite arm spacing, the grain size and the local solidification time. Assuming negligible diffusion in the solid state during casting, the composition profile of the alloying elements can be described with the Scheil equation:

$$C_s = C_0 \cdot K \cdot (1 - f_s)^{K-1} \quad (1)$$

where,  $C_0$  the alloy nominal composition,  $K$  the partition coefficient and  $C_s$  the element composition when the solid weight fraction is  $f_s$ . The Scheil calculations for a multicomponent alloy system can be performed with the THERMOCALC software.

These calculations were performed under the following assumptions:

- Complete mixing in the liquid state.
- No diffusion in the solid state (also known as the Scheil condition).
- Thermodynamic equilibrium at the solid/liquid interface.

The assumption of negligible diffusion in the solid is acceptable due to the short local solidification time at industrial direct-chill casting conditions.

The solidification path is depicted in Fig. 2 as the temperature vs. the weight fraction of solid phases formed. The arrows in Fig. 2 indicate the starting temperature for the formation of various solid phases during solidification. The first phase to form is the matrix FCC phase at the liquidus temperature of 655 °C. The phase sequence during solidification is therefore FCC → α-AlFeSi → β-AlFeSi → Mg<sub>2</sub>Si → Si-diamond. The solidus temperature is 557 °C.

In order to calculate the concentration profiles of alloying elements as well as the weight fraction profiles of solid phases, the

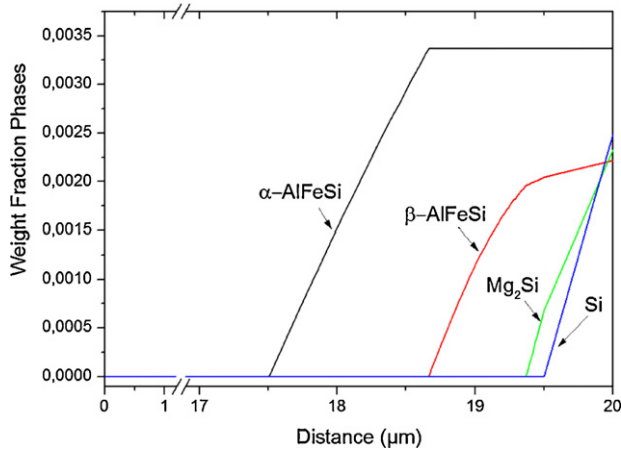


Fig. 3. Weight fraction profiles of solid phases (FCC matrix not included) after solidification.

fraction solid axis  $f_s$  was converted to a distance axis  $x_s$  via the relation

$$x_s = f_s \frac{d}{2} \quad (2)$$

where  $d$  is the mean grain size after solidification. It should be noted that Eq. (2) provides a one-dimensional approximation of the solute profiles.

For a mean grain size of 40  $\mu\text{m}$  considered here, the value  $x_s = 0$  corresponds to the grain center and the value  $x_s = 20$  corresponds to the grain boundary.

The profiles of weight-fractions of solid phases that form in addition to the major aluminum matrix FCC phase during solidification are shown in Fig. 3. All phases form in the vicinity or at the grain boundary as expected. The corresponding profiles of alloying elements in solution in the aluminum matrix (FCC phase) are shown in Fig. 4. A high degree of microsegregation is evident. The Mg concentration in FCC drops close to the grain boundary due to the formation of  $\text{Mg}_2\text{Si}$ . In Fig. 5, which is a close up of Fig. 4, the profiles of Fe and Mn are shown. Again the Fe profile exhibits a drop due to the formation of the iron intermetallics, i.e. the  $\alpha\text{-AlFeSi}$  and  $\beta\text{-AlFeSi}$  phases.

### 3.2. Homogenization—problem set-up

The homogenization heat treatment can be simulated as a diffusion–precipitation process. The following phenomena take

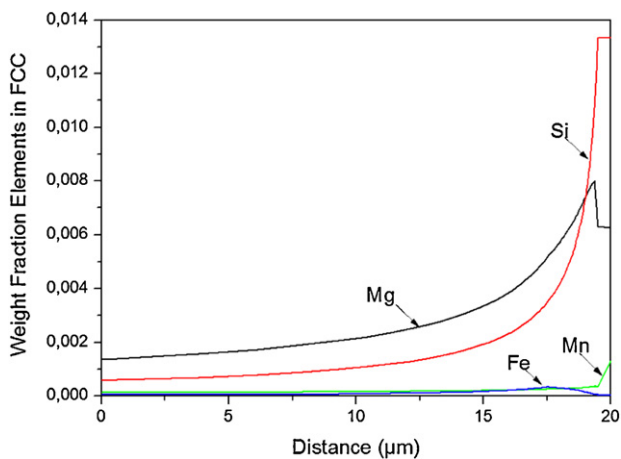


Fig. 4. Profiles of alloying elements in the FCC matrix phase after solidification.

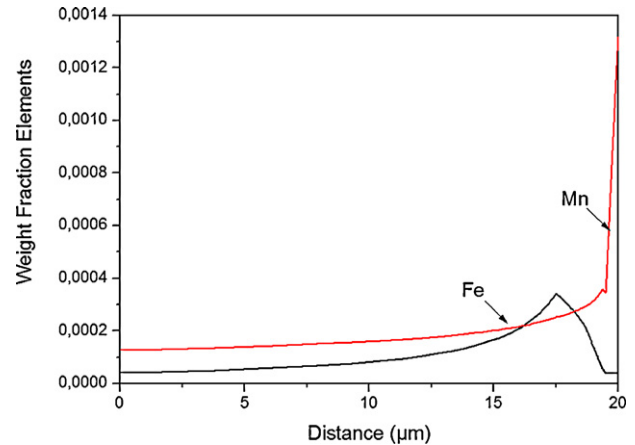


Fig. 5. A magnification of Fig. 4 showing profiles of Fe and Mn in the FCC matrix phase after solidification.

place simultaneously, (a) removal of microsegregation, (b) phase dissolution and (c) precipitation inside the grains. Bulk diffusion or precipitation/dissolution reactions control the overall kinetics (Robson and Prangnell, 2003), depending on the temperature and the diffusion length. For the complete definition of the as-cast microstructure the following information is needed:

- Initial concentration profiles of the alloying elements.
- Secondary phases weight fraction.
- Secondary phases morphology within the grains.
- Thermal cycle of homogenization.
- A geometric model where the diffusion equations will be solved.

The initial concentration profiles and the weight fraction of secondary phases are the results from the Scheil calculations (Figs. 3–5). The thermal cycle is an operational parameter having as an upper limit the eutectic temperature. An appropriate geometric model was considered for the description of the homogenization heat treatment, shown in Fig. 6. Due to symmetry, only half of the grain was considered. The  $\text{Mg}_2\text{Si}$  and the  $\alpha\text{-AlFeSi}$  are taken as dispersed phases in the FCC matrix. The  $\beta\text{-AlFeSi}$  phase is taken as a region attached to the right of the FCC matrix at the grain boundary. As stated in Section 2 this diffusion problem was solved with the computational kinetics package DICTRA. The DICTRA module for diffusion in dispersed systems treats problems involving diffusion through microstructures containing dispersed precipitates of secondary phases. Diffusion is assumed to take place only in the matrix phase. The dispersed phases act as point sinks or sources of solute atoms in the simulation and their fraction and composition is calculated from the average composition in each node, assuming that equilibrium holds locally in each volume element. This

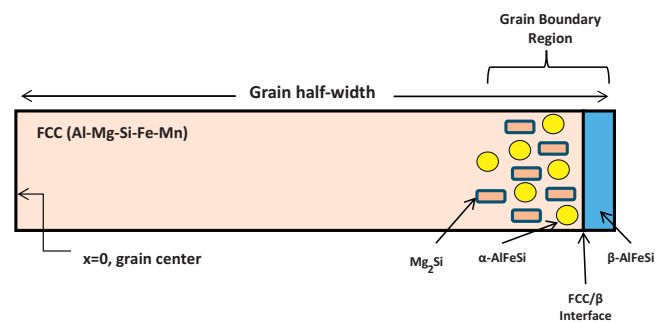


Fig. 6. The geometrical model adopted for the simulation of homogenization process.

module is suitable for long-range diffusion calculations compared with the inter-particle distances. The basic model assumption is that the growth and dissolution rates are very high compared with the diffusion rates in the matrix. Alternatively, the matrix diffusion is the controlling mechanism of the overall kinetics. This assumption is tolerable for the high homogenization temperatures, since the growth-dissolution rates are very high and the particles reach the equilibrium state very fast. Consequently the local conditions are rather concentration-dependent than time-dependent. Locally, most of the solute is trapped into the particles, reducing the concentration gradients and the diffusion rate in the matrix.

The homogenization simulations were carried out under the following assumptions:

- One-dimensional geometry (planar geometry).
- All major elements included in the simulation (Al–Mg–Si–Fe–Mn).
- The effect of formation or dissolution of intermetallic phases during the homogenization on the composition profiles of the alloying elements has been taken into account.
- The diffusivities of the alloying elements are both temperature and composition dependent.

As stated above in Section 2, the homogenization problem was divided computationally in two steps (2 and 3). In step 2 the simulation of the dissolution of  $Mg_2Si$  during homogenization and its subsequent re-precipitation during cooling was performed. The results are presented below in Section 3.3. In step 3, the simulation of the  $\beta$ -AlFeSi  $\rightarrow$   $\alpha$ -AlFeSi was performed. This transformation was monitored by the movement of the FCC/ $\beta$  interface (see Fig. 6) and the resulting increase of the weight fraction of the dispersed  $\alpha$ -AlFeSi phase. The width of the  $\beta$ -AlFeSi region was calculated relative to the grain half-width. In order to do this, the volume fraction of the  $\beta$  phase was calculated from the weight fraction profile of Fig. 3. The volume fraction was then normalized over the grain half-width. The width of the  $\beta$ -AlFeSi region in Fig. 6 is, therefore, grain size dependent. The results of the simulations are presented in Section 3.4.

### 3.3. Dissolution of $Mg_2Si$

The first step of the homogenization process involves the dissolution of the  $Mg_2Si$  phase from the grain boundaries and its re-precipitation in the grain interiors during cooling from the homogenization temperature. In the DICTRA program the  $Mg_2Si$  phase was entered as a dispersed phase with the volume fraction profile given in Fig. 3. This profile is a result of a Scheil simulation, shown earlier in Section 3.1 and is saved as an input file for the  $Mg_2Si$  volume fraction to be read by DICTRA. The profiles of all alloying elements, shown in Fig. 4 were also entered from input files in the DICTRA program. The thermal cycle for the simulation involved isothermal holding at 540–580 °C up to 10 h and then air cooling to room temperature in 2 h. The reduction of the weight fraction of  $Mg_2Si$  during homogenization at 540 °C is shown in Fig. 7. The  $t=0$  curve is the  $Mg_2Si$  profile at the beginning of homogenization. As seen in Fig. 7, the  $Mg_2Si$  phase dissolves rapidly and the complete dissolution of  $Mg_2Si$  takes only about 15 min at 540 °C. Therefore the literature reports by Cai et al. (2002) as well as by Kuijpers (2004) that  $Mg_2Si$  dissolution is fast is confirmed by these calculations. The  $Mg_2Si$  phase is precipitated during cooling from the homogenization temperature in the grain interior. This is shown by the straight line in the top of Fig. 7 and is in agreement with the re-precipitation of  $Mg_2Si$  observed experimentally by Mrówka-Nowotnik and Sieniawski (2005) who studied the effect of cooling rate following homogenization on the properties of Al–Mg–Si alloys. The nucleation of  $Mg_2Si$  is handled in

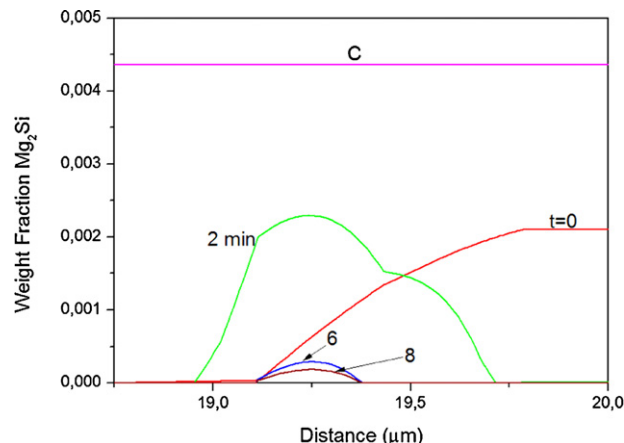


Fig. 7. The dissolution of  $Mg_2Si$  during homogenization. The  $t=0$  curve is the  $Mg_2Si$  profile at the start of homogenization and the curve labeled C at the top is after cooling from the homogenization temperature.

DICTRA thermodynamically, that is the program monitors continuously the precipitation driving force and allows the formation of the phase when this value turns positive. This re-precipitation of  $Mg_2Si$  within the grains aids the dissolution of this phase during preheating in the extrusion shop and enhances the response of the alloy to the aging treatment following the extrusion of the billets.

The Mg and Si profiles in the Al FCC matrix phase following the dissolution of the  $Mg_2Si$  phase are shown in Fig. 8. The  $t=0$  curve corresponds to the initial profiles before homogenization. After homogenization the profiles are uniform and all segregation has been removed.

### 3.4. Transformation $\beta$ -AlFeSi $\rightarrow$ $\alpha$ -AlFeSi during homogenization

#### 3.4.1. Comparison with experimental data

As stated in Section 3.2, the transformation is monitored by the movement of the FCC/ $\beta$  interface (see Fig. 6) and the resulting increase of the weight fraction of the dispersed  $\alpha$ -AlFeSi phase. The transformed fraction is given as a function of homogenization time for homogenization temperatures of 540–580 °C in Fig. 9. In the same figure the experimental data from Kuijpers et al. (2005) for the 6063 alloy are included for comparison. They determined the transformed fraction by measuring the (Fe + Mn)/Si ratio of particles by means of SEM/EDX technique. This technique in distinguishing between  $\alpha$ - and  $\beta$ -AlFeSi is however not very accurate, introduces

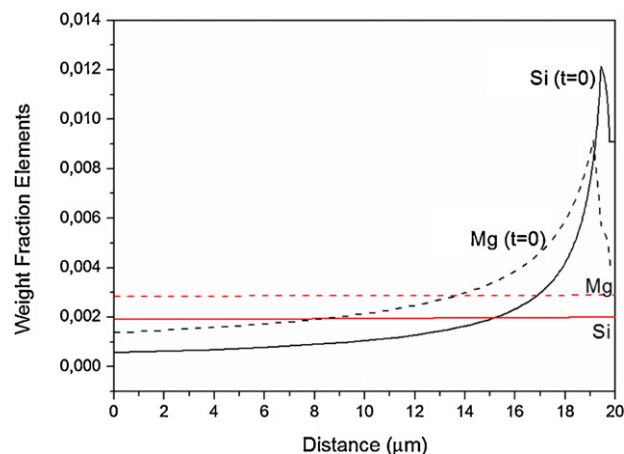
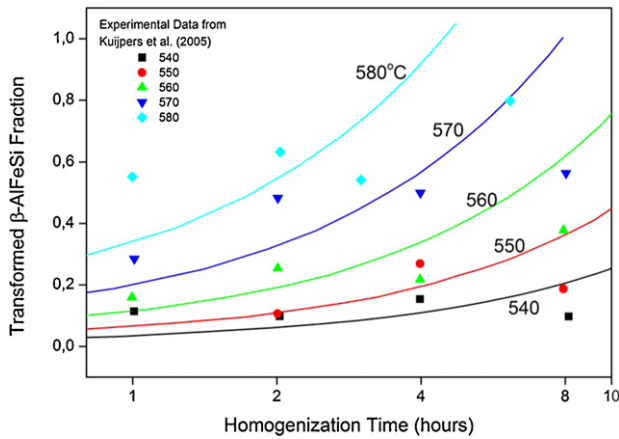
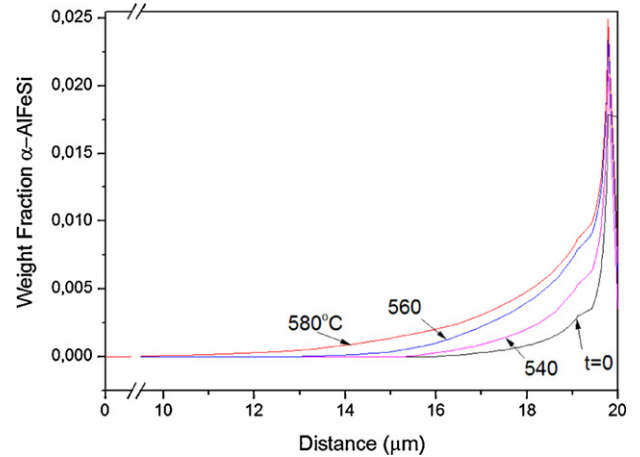


Fig. 8. Mg and Si profiles in the FCC matrix phase at the beginning and at the end of homogenization.



**Fig. 9.** The fraction of transformation  $\beta$ -AlFeSi  $\rightarrow$   $\alpha$ -AlFeSi as a function of homogenization temperature and time. Points are experimental data from Kuijpers et al. (2005).



**Fig. 12.** Evolution of the  $\alpha$ -AlFeSi phase profile as a function of homogenization temperature for 10 h homogenization time.

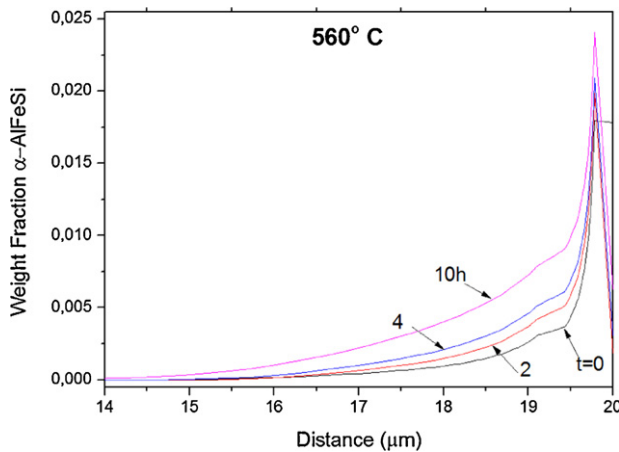


**Fig. 10.** Evolution of the  $\alpha$ -AlFeSi phase profile as a function of homogenization time at 560 °C.

uncertainties and provides several irrational data points. The model predicts the general trend of the increasing transformation fraction with homogenization time and also predicts well the kinetics of the transformation. Compared to the experimental data, the model predicts lower transformed  $\beta$ -fraction at short homogenization times and higher transformation at longer homogenization times. Taking into account the uncertainties of the experimental measurement of  $\beta$  to  $\alpha$  transformation as discussed by Kuijpers et al. (2003b), the

fact that some experimental points are irrational (e.g. at 580 °C the point at 3 h is lower than the previous point at 2 h homogenization time), as well as the assumptions, on which the present model was based, we can conclude that the agreement between model and experimental data is reasonable.

### 3.4.2. Evolution of $\alpha$ -AlFeSi phase fraction during homogenization

As the  $\beta \rightarrow \alpha$  transformation proceeds, the fraction of  $\alpha$ -phase increases. The model is able to calculate the profile of the  $\alpha$ -phase across the grain. The results are given in Fig. 10 as a function of homogenization time at 560 °C homogenization temperature. The  $t = 0$  curve corresponds to the profile of the  $\alpha$ -AlFeSi phase present at the start of homogenization (end of solidification). It is evident that additional  $\alpha$ -AlFeSi phase forms during the course of homogenization and that the profile of  $\alpha$ -AlFeSi spreads toward the grain interior. The evolution of the profiles of Fe and Mn in the FCC phase at 560 °C are given in Fig. 11a and b respectively. The concentration profiles become more uniform with the homogenization time. For distances above  $x_s = 15 \mu\text{m}$  the concentration profiles become even out due to the formation of the  $\alpha$ -AlFeSi phase.

In order to assess the effect of homogenization temperature, the profiles of  $\alpha$ -AlFeSi phase for 10 h homogenization time are given as a function of homogenization temperature in Fig. 12. It is evident that higher amount of  $\alpha$ -AlFeSi phase forms at higher homogenization temperatures and the weight fraction profile spreads toward the grain interior. The corresponding profiles of Fe and Mn in the FCC phase are shown in Fig. 13a and b respectively. The arrows in

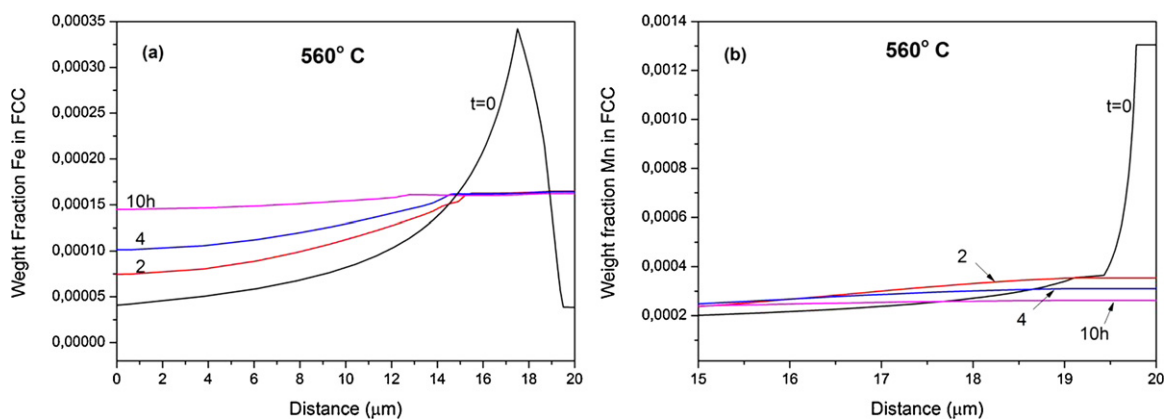


**Fig. 11.** Evolution of (a) Fe and (b) Mn profiles in FCC matrix phase as a function of homogenization time at 560 °C.

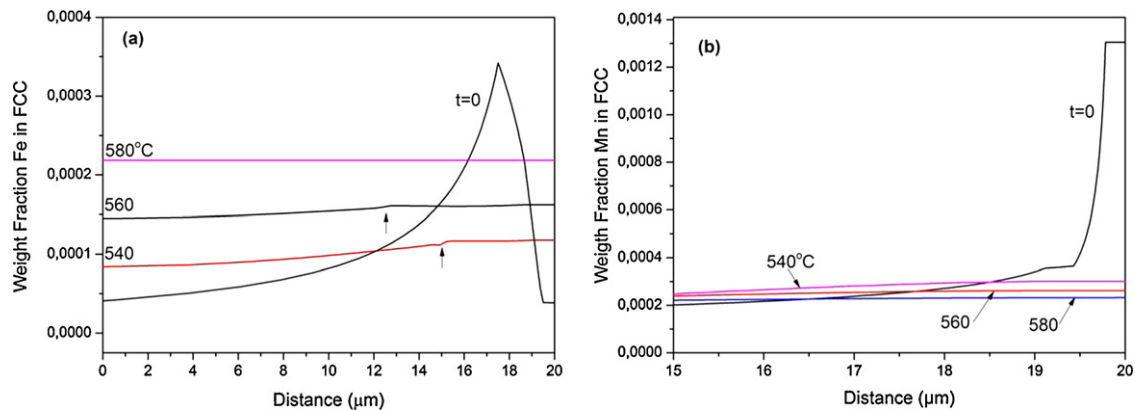


Fig. 13. Evolution of (a) Fe and (b) Mn profiles in FCC matrix phase as a function of homogenization temperature for 10 h homogenization time.

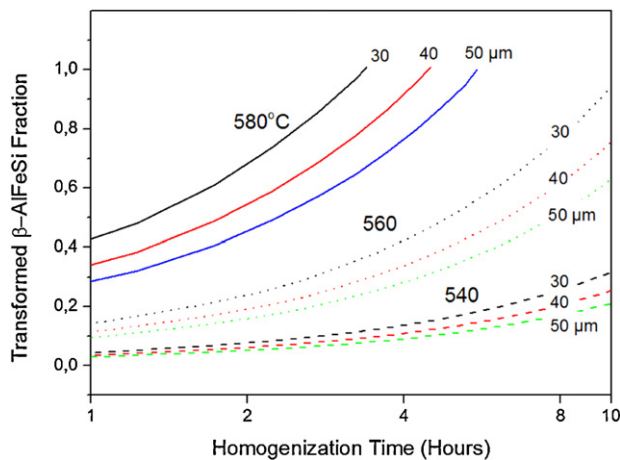


Fig. 14. Effect of grain size on transformation of  $\beta$ -AlFeSi  $\rightarrow$   $\alpha$ -AlFeSi for three homogenization temperatures.

Fig. 13a indicate the distance where the  $\alpha$ -AlFeSi phase starts to form.

#### 3.4.3. Effect of grain size

Grain size influences the transformation kinetics since it controls the distance over which diffusion of alloying elements takes place. The effect of grain size is introduced through Eq. (2) in Section 3.1. Calculations were performed for three grain sizes 30, 40 and 50  $\mu\text{m}$ . The results are shown in Fig. 14 which depicts the transformation of  $\beta$ -AlFeSi to  $\alpha$ -AlFeSi as a function of homogenization time, for three homogenization temperatures 540, 560 and 580  $^{\circ}\text{C}$ . The transformation is faster the smaller the grain size, due to the shorter diffusion distances, and the effect is larger at higher homogenization temperatures.

## 4. Conclusions

The work described in this article presented a method for the computational simulation of the  $\beta$ -AlFeSi to  $\alpha$ -AlFeSi transformation during the homogenization of 6xxx extrudable aluminum alloys. This was achieved with the computational integration of the process steps of solidification and homogenization. The composition profiles of alloying elements as well as the weight fraction profiles of all solid phases, computed after solidification, were entered as input for the simulation of the homogenization process which involved the dissolution of the  $\text{Mg}_2\text{Si}$  and the transformation of  $\beta$ -AlFeSi to  $\alpha$ -AlFeSi intermetallics. The transformation fraction

was computed as a function of homogenization temperature and time and the transformation kinetics compared well with published experimental data. The evolution of  $\alpha$ -AlFeSi weight fraction profile and the effect of grain size on transformation kinetics were also evaluated. The results indicate that the simulation might be a valuable tool for the design of the homogenization treatment of these alloys.

## Acknowledgements

This work has been performed in the framework of cooperation with Aluminium of Greece (AoG). Fruitful discussions with E. Grigoriou of AoG are greatly appreciated.

## References

- Andersson, J.O., Helander, T., Höglund, L., Shi, P., Sundman, B., 2002. Thermo-Calc & DICTRA, computational tools for materials science. *Calphad—Computer Coupling of Phase Diagrams and Thermochemistry* 26, 273–312.
- Borgenstam, A., Höglund, L., Ågren, J., Engström, A., 2000. DICTRA, a tool for simulation of diffusional transformations in alloys. *Journal of Phase Equilibria* 21, 269–280.
- Cai, M., Robson, J.D., Lorimer, G.W., Parson, N.C., 2002. Simulation of the casting and homogenization of two 6xxx series alloys. *Materials Science Forum* 396–402, 209–214.
- Kuijpers, N.C.W., Vermolen, F.J., Vuurk, K., van der Zwaag, S., 2003a. A model of the  $\beta$ -AlFeSi to  $\alpha$ -Al(FeMn)Si transformation in Al—Mg—Si alloys. *Materials Transactions* 44, 1448–1456.
- Kuijpers, N.C.W., Kool, W.H., Koenis, P.T.G., Nilsen, K.E., Todd, I., van der Zwaag, S., 2003b. Assessment of different techniques for quantification of  $\alpha$ -Al(FeMn)Si and  $\beta$ -AlFeSi intermetallics in AA 6xxx alloys. *Materials Characterization* 49, 409–420.
- Kuijpers, N.C.W., 2004. Kinetics of the  $\beta$ -AlFeSi to  $\alpha$ -Al(FeMn)Si transformation in Al—Mg—Si alloys. PhD Thesis. TU Delft. 79–101.
- Kuijpers, N.C.W., Vermolen, F.J., Vuurk, C., Koenis, P.T.G., Nilsen, K.E., Zwaag, S.v.d., 2005. The dependence of the  $\beta$ -AlFeSi to  $\alpha$ -Al(FeMn)Si transformation kinetics in Al—Mg—Si alloys on the alloying elements. *Materials Science and Engineering A* 394, 9–19.
- Liu, Y.L., Kang, S.B., 1997. The solidification process of Al—Mg—Si alloys. *Journal of Materials Science* 32, 1443–1447.
- Mrówka-Nowotnik, G., Sieniawski, J., 2005. Influence of heat treatment on the microstructure and mechanical properties of 6005 and 6082 aluminium alloys. *Journal of Materials Processing Technology* 162–163, 367–372.
- Mrówka-Nowotnik, G.S., Wierzbńska, J.M., 2007. Intermetallic phase particles in 6082 aluminium alloy. *Archives of Materials Science and Engineering* 28, 69–76.
- Onurlu, S., Tekin, A., 1994. Effect of heat treatment on the insoluble intermetallic phases present in an AA 6063 alloy. *Journal of Materials Science* 29, 1652–1655.
- Robson, J.D., Prangnell, P.B., 2003. Modelling Al<sub>3</sub>Zr dispersoid precipitation in multicomponent aluminium alloys. *Materials Science and Engineering A* 352, 240–250.
- Samaras, S.N., Haidemenopoulos, G.N., 2007. Modelling of microsegregation and homogenization of 6061 extrudable Al-alloy. *Journal of Materials Processing Technology* 194, 63–73.
- Tanihata, H., Sugawara, T., Matsuda, K., Ikeno, S., 1999. Effect of casting and homogenizing treatment conditions on the formation of Al—Fe—Si intermetallic compounds in 6063 Al—Mg—Si alloys. *Journal of Materials Science* 34, 1205–1210.